Integrating Artificial Neural Networks with Geospatial Analysis to Forecast Future Urban Flood Risk in the Dam-Regulated Shiroro Catchment, Niger State

Chukwu S. & *Adesina E.A.
Department of Surveying and Geoinformatics, Federal University of Technology, Minna
*Corresponding author**:** adegeoworldsolutions@gmail.com

Received: 12/11/2025 **Revised:** 3/12/2025 **Accepted:** 15/12/2025

Urban flood risk in dam-regulated catchments is a dynamic and escalating challenge, driven by the interplay of hydrological modifications, land use change, and climate variability. This study develops and validates a forecasting framework that integrates Artificial Neural Networks (ANN) with geospatial analysis to project future urban flood risk in the Shiroro Dam catchment, Niger State, Nigeria. The framework synergistically combines urban growth simulation, climate change Scenarios, and an ANN model trained on topographic, climatic, land cover, and soil moisture variables. Analysis of multi-temporal Landsat imagery (2014-2024) revealed significant landscape transformation, including substantial agricultural loss and water body expansion due to dam impoundment. The ANN model demonstrated superior predictive performance (accuracy: 91.6%; Kappa: 82%) compared to traditional GIS-overlay methods. It identified 35.06% of the study area as highly vulnerable to flooding, with population densities in risk zones projected to reach 7,318 persons/km² by 2034. The study provides a robust, transferable tool for proactive flood risk management, emphasizing the need for integrated land-use planning and offering a scalable methodology for other dam-affected catchments.
Keywords: Artificial Neural Network; CA-Markov; climate change; dam-induced flooding; flood risk assessment; geospatial analysis; remote sensing; urban growth modelling

Introduction

Flooding constitutes one of the most devastating and widespread natural hazards globally, accounting for nearly half of all weather-related disasters (UNISDR, 2017; Adesina *et al.,* 2025). The frequency and magnitude of flood events are projected to intensify under the influence of climate change, which is altering precipitation patterns and increasing the frequency of extreme rainfall events (IPCC, 2022). This escalating physical hazard is compounded by rapid and often unplanned urbanization, which places more people and assets in harm's way. Consequently, the global population exposed to flood risks is expected to rise significantly, with estimates suggesting up to 1.6 billion people could be vulnerable by 2050, particularly in low-lying and rapidly developing regions (Dottori *et al.,* 2018).

This global challenge is acutely manifested in Nigeria, a country ranked among the most vulnerable to flood disasters in Africa. The nation has experienced recurrent catastrophic events, such as the widespread flooding in 2012 and 2022, which resulted in thousands of fatalities, displaced millions of people, and inflicted billions of dollars in damage to infrastructure and agricultural lands (NKwunonwo *et al.,* 2020; EM-DAT, 2023; Adesina *et al.,* 2021). The situation in Nigeria exemplifies the critical convergence of climate vulnerability and socio-economic exposure that characterizes flood risk in the developing world.

Within Nigeria, the Niger State region, home to the Shiroro Dam, represents an area of concern due to a unique set of compounding risks. The Shiroro Dam is a cornerstone of the nation's energy infrastructure, providing vital hydroelectric power, while its reservoir supports irrigation and local livelihoods (Adepoju *et al.,* 2020). However, the operation of large dams like Shiroro creates a paradoxical situation. During periods of intense rainfall, controlled releases through the spillways are necessary to maintain the structural integrity of the dam. These managed releases, however, can result in sudden and amplified downstream flooding, for which riparian communities are often unprepared (Abubakar *et al.,* 2018; Okonkwo *et al.,* 2021; Adesina *et al.,* 2025).

This dam-induced hazard is severely exacerbated by concurrent rapid, unplanned urban expansion. Driven by population growth and economic pressure, settlements in cities like Minna and surrounding peri-urban areas are increasingly encroaching upon natural floodplains and drainage channels (Adesina *et al.,* 2025; Olanrewaju *et al.,* 2019). This unchecked development, frequently occurring without adequate drainage infrastructure, increases surface runoff and directly places homes, businesses, and infrastructure in the path of floodwaters (Gupta *et al.,* 2020). Therefore, the interplay of dam operations and unsustainable land use practices creates a unsafe feedback loop of rising flood risk, demanding advanced predictive modelling to inform future planning and mitigate impending disasters.

Current flood hazard assessments in the Shiroro region and similar contexts often rely on static, historical data and conventional methodologies such as GIS-overlay analysis or hydrological models like HEC-RAS (Olanrewaju *et al.,* 2019; Nkwunonwo *et al.,* 2020). While valuable, these methods face a

crucial limitation. First, they often fail to capture the non-linear and complex interactions between climatic variables, hydrological processes, and land use dynamics, which jointly influence flood genesis and impact. Second, and more fundamentally, they are predominantly retrospective, lacking the capacity to proactively incorporate future drivers of risk. Most existing studies do not account for projected urban expansion, a major driver of exposure as settlements continue to grow into flood-prone areas. They also rarely integrate future climate change projections that will alter the hydrological regime (Adesina *et al.,* 2021). Moreover, there is limited research focusing on dam-regulated catchments in Africa, where dam operations significantly modulate flood regimes.

Globally, machine learning (ML) models have demonstrated a superior ability to analyse large datasets, uncover complex relationships, and generate highly accurate flood susceptibility maps (Mosavi *et al.,* 2018; Shahabi *et al*., 2021). However, in Nigeria and specifically within dam-influenced catchments, the application of ML for predictive flood risk assessment remains largely underexplored. A critical disconnect exists between three advanced fields: urban growth modelling (UGM), climate change projection, and ML-based hydrology. While each field is mature in isolation, their integration into a unified forecasting framework is scarce. Specifically, there is a conspicuous absence of a methodology that can simulate how future urban landscapes, under changing climatic conditions, will interact with the specific hydrological regime of a dam-controlled watershed to reshape future flood risk.

Therefore, this study aims to fill this gap by developing and validating a novel, integrative forecasting framework for the Shiroro Dam catchment. This research develops a dynamic forecasting framework that integrates: (i) urban expansion projections, (ii) climate change Scenarios to modify extreme rainfall inputs, and (iii) an Artificial Neural Network (ANN)-based flood hazard model. This framework is applied to map future urban flood vulnerability for the year 2034 under combined land-use and climate change Scenarios. The future climate projections will be used to generate potential extreme rainfall events, which will serve as modified inputs to the trained ANN model to forecast flood hazard under changing climate conditions. The primary objective is to identify urban areas at high risk under projected future Scenarios, thereby providing an evidence base for proactive disaster risk reduction and sustainable land-use planning and contributing directly to the academic discourse on dynamic risk assessment.

Materials and Methods

Study area

The study focuses on the Shiroro Dam region in Niger State, Nigeria, geographically bounded by latitudes 9°55'N to 10°10'N and longitudes 6°30'E to 6°45'E (Figure 1). The area encompasses the dam's immediate catchment and downstream settlements, including Shiroro Town, Gwada, Kuta, and the peri-urban fringes of Minna, which have a documented history of periodic flooding. The region features a mixed landscape of rural agrarian communities and rapidly expanding peri-urban settlements, with population growth rates averaging 2.8-3.5% per annum. The recent commissioning of the Zungeru Hydropower Dam upstream introduces an additional layer of complexity to the catchment's hydrology, making it a critical area for flood risk investigation. The selection of this catchment is justified by its representative combination of dam-regulated hydrology, rapid urbanization, and documented flood history, providing an ideal case for testing an integrated forecasting framework.

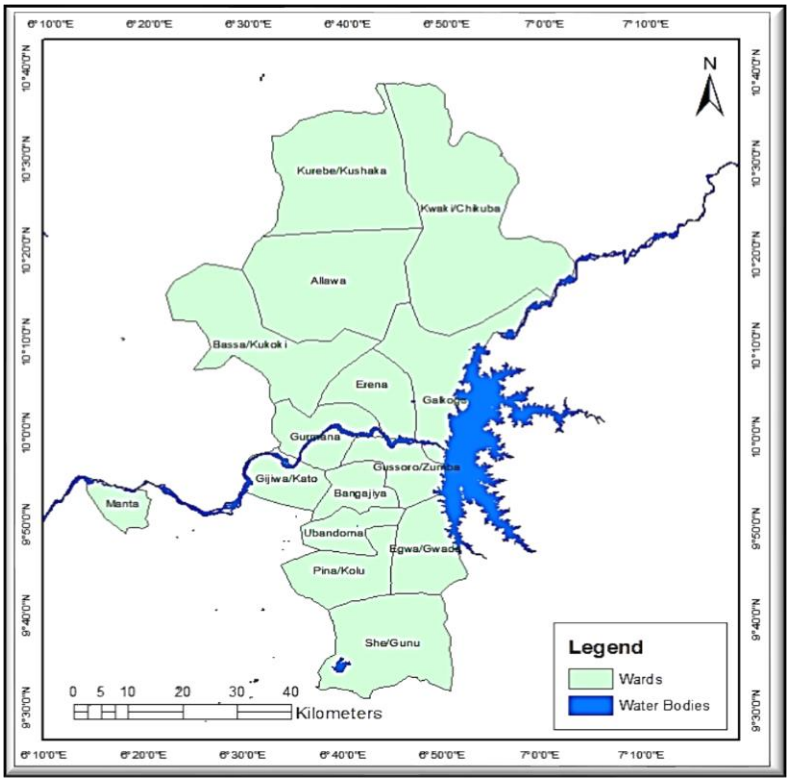

Figure 1: **Map of the study area**

Data acquisition and pre-processing

A multi-source geospatial dataset was acquired to support the integrated modelling approach. All raster datasets were pre-processed to a consistent spatial resolution (30 m) and coordinate system (WGS 84 UTM Zone 32N) to ensure analytical integrity. The key datasets are summarized in Table 1.

Table 1: Data types, specifications, and sources

S/N	Data Type	Spatial Resolution	Temporal Coverage / Acquisition Date(s)	Source	Justification for Selection
1	Landsat 8/9 OLI/TIRS Imagery	30 m	2014, 2024	USGS Earth Explorer	Provides consistent, multi-spectral data for LULC classification and change detection over the study period.
2	TanDEM-X DEM	12 m	2018	DLR Earth Observation Centre	High-resolution elevation data critical for deriving slope, flow accumulation, and topographic wetness index, key factors in flood modelling.

S/N	Data Type	Spatial Resolution	Temporal Coverage / Acquisition Date(s)	Source	Justification for Selection
3	Gridded Population Density	100 m	2023	GRID3, NASRDA	Spatially explicit population data essential for exposure assessment and as a driver in urban growth modelling.
4	Rainfall Data	Point (Stations)	Daily (2014-2024)	Nigerian Meteorological Agency (NIMET)	Historical rainfall records required for training the ANN and establishing baseline climate conditions.
5	Historical Flood Extent	-	2022	National Emergency Management Agency (NEMA)	Ground truth data for model training and validation.
6	Administrative Boundaries	-	-	OSGOF	For zonal analysis and reporting.
7	Soil Moisture Index	30 m	2014, 2024	Derived from Landsat 8/9 TIRS and OLI bands using the Normalized Difference Water Index (NDWI)	Indicator of antecedent soil conditions affecting runoff generation.

Data pre-processing followed a standardized workflow to ensure consistency across all geospatial datasets. For the Landsat imagery, atmospheric correction was performed using the Semi-Automatic Classification Plugin (SCP) in QGIS 3.44 version, followed by geometric alignment and masking to the study area boundary. Cloud cover was minimal (<10%), and affected pixels were masked using the Quality Assessment (QA) band. The TanDEM-X DEM was processed to derive slope and topographic wetness index maps, which are for hydrological modelling. Station-based rainfall data were spatially interpolated into continuous raster surfaces using Ordinary Kriging. It is acknowledged that uncertainties in rainfall interpolation, due to station distribution, and potential vertical errors in the DEM (estimated at ~2 m) constitute limitations of the dataset.

The research methodology, illustrated in Figure 2, was structured around three core integrated components to form a dynamic forecasting chain: (1) historical analysis and projection of LULC, (2) ANN-based flood hazard modelling trained on historical data, and (3) assessment of future population exposure by integrating the outputs of the first two components under climate change scenarios. The logic integrates the outputs of one component as inputs to the next, creating a cohesive forecasting pipeline.

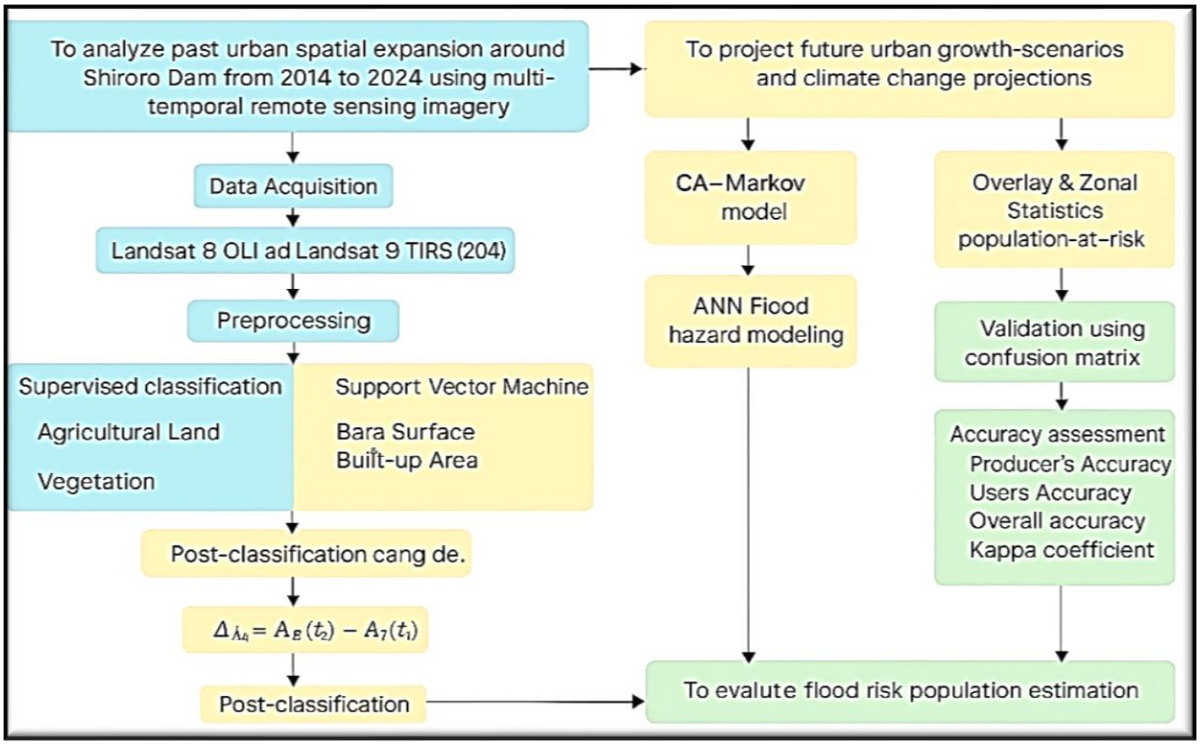

Figure 2: Methodology flow diagram

Land use/land cover classification and change detection

Multi-temporal Landsat images for 2014 and 2024 were classified using a supervised classification algorithm (Maximum Likelihood) in ArcGIS Pro 3.4.4. While Maximum Likelihood is a well-established method, its use here is justified by its computational efficiency and satisfactory performance given the study's focus on broad LULC classes. Future work could employ machine learning classifiers for comparison. Training samples were meticulously collected for five LULC classes: Agricultural Land, Bare Surface, Built-up Area, Dense Vegetation, and Water Bodies. Post-classification change detection was applied using raster algebra to quantify the net change (ΔA_k) for each class between 2014 and 2024, a standard metric for assessing LULC dynamics (Lu and Weng, 2007). The net change was calculated using Equation (1):

$$\Delta A_k = A_k(t_2) - A_k(t_1) \quad (1)$$

where $A_k(t_2)$ and $A_k(t_1)$ are the areas of class k at the final (2024) and initial (2014) time steps, respectively. Accuracy assessment was performed using 200 stratified random points. The overall accuracy was 88.5% with a Kappa coefficient of 0.84. Class-specific user's and producer's accuracies ranged from 82% to 94%.

Future urban growth and LULC projection

Future LULC for 2034 was simulated using the Cellular Automata-Markov (CA-Markov) model, implemented within the Modules for Land Use Change Evaluation (MOLUSCE) plugin in QGIS 3.44. The classified LULC maps of 2014 and 2024 served as inputs to compute transition probability matrices and areas. Key spatial drivers of change, including Euclidean distance from roads and rivers, elevation, and population density, were integrated. These drivers were selected based on empirical evidence from the region indicating their influence on settlement expansion and land conversion (Olanrewaju *et al.,* 2019). An Artificial Neural Network within MOLUSCE (configured with a single hidden layer of 10 neurons and a learning rate of 0.01) was employed to model the non-linear relationships between these drivers and land transition potentials. The CA-Markov model then used these potentials to project the 2034 LULC under a business-as-usual Scenario.

To assess the reliability of the projection model, a standard hindcast validation was performed. The model was validated by simulating the 2024 LULC using the 2014 map as a baseline. The simulated 2024 map was then compared to the actual 2024 classified map using a confusion matrix. This validation yielded a Kappa statistic of 0.78, indicating substantial agreement between the simulated and actual LULC (Vanbelle *et al.,* 2024). This level of agreement supports the use of the calibrated model for projecting the 2034 LULC scenario, acknowledging its foundation on current trends.

Flood hazard mapping using Artificial Neural Network (ANN)

Five causative factors were selected based on their established influence on flood genesis in dam-regulated catchments: rainfall, elevation, slope, soil moisture index, and land use/land cover (LULC). These factors were normalized to a common scale (0-1) before being fed into the ANN. The descriptive statistics and data sources for the continuous input factors are summarized in Table 2. The fifth input factor, LULC, was a categorical variable derived from the 2024 classification and was one-hot encoded.

Table 2: Descriptive statistics of the continuous input factors used in the ANN model

Factor	Min Value	Max Value	Mean	Std. Dev.	Source
Rainfall (mm/yr)	1,710	2,320	2,010	145.6	NIMET
Elevation (m)	121	731	412.3	132.5	TanDEM-X
Slope (°)	0	65.8	12.4	8.9	Derived from TanDEM-X
Soil Moisture Index	0.001	0.99	0.45	0.21	Derived from Landsat (NDWI)

A flood inventory map was created from the documented 2022 flood extent obtained from NEMA. From this inventory, 600 flood points were randomly generated within the inundated areas. An equivalent 600 non-flood points were generated from areas confirmed to be dry in 2022 and in historical records, ensuring stratification across all LULC and topographic classes. The total sample size of 1,200 points, while limited, was deemed sufficient for initial model development given the study area's homogeneity in flood-driving factors. To address potential spatial autocorrelation, a minimum distance constraint of 500m was applied during point generation. The model was trained on this dataset, randomly split into 70% for training, 15% for validation, and 15% for testing. A 5-fold cross-validation was also performed, yielding a mean accuracy of 90.2% (±1.8%), confirming model stability.

The ANN architecture consisted of an input layer (5 neurons), two hidden layers with 12 and 8 neurons respectively (using ReLU activation), and a single output neuron with a sigmoid activation function to produce a flood probability between 0 and 1. The architecture (5-12-8-1) was determined through iterative testing to optimize performance while minimizing complexity. The Adam optimization algorithm was used with a learning rate of 0.001, and early stopping was implemented to prevent overfitting. A sensitivity analysis confirmed that model performance was not unduly influenced by the chosen normalization method. The resultant probability map was classified into three hazard zones: 'Low/Very Low', 'Moderate', and 'High/Very High'.

Population exposure analysis and model validation

The population at risk (P_{risk}) was estimated by overlaying the classified flood hazard map with a gridded population density layer using zonal statistics, following the standard exposure assessment methodology which multiplies hazard area by population density to estimate headcount (Jongman *et al.*, 2012). The calculation was performed using Equation (2):

$$P_{risk} = \sum_{i=1}^{n}(A_i * D_i) \qquad (2)$$

The population at risk (P_{risk}) was estimated using zonal statistics: $P_{risk} = \sum_{i=1}^{n}(A_i * D_i)$; where A_i is the area of flood hazard zone i, and D_i is the mean population density within that zone.

The predictive performance of the ANN model was thoroughly validated by comparing its classified hazard map against the independent, observed 2022 flood extent from NEMA. A confusion matrix was constructed, and standard classification metrics, Accuracy, Precision, Recall, F1-Score, and Kappa Index, were calculated to quantitatively benchmark the ANN against a traditional multi-criteria GIS-overlay (baseline) method.

Integration of future climate and population scenarios

To forecast flood hazard for the year 2034, the trained ANN model was applied using modified inputs that represent projected future conditions. This involved two key updates: (1) **Land Use/Land Cover (LULC):** The historical LULC map was replaced with the 2034 LULC projection simulated by the CA-

Markov model (Section 2.3.2). (2) **Climate Input (Rainfall):** To incorporate climate change, future rainfall inputs were developed using regional climate projections. Bias-corrected data from the CORDEX-Africa ensemble for two representative concentration pathways, RCP 4.5 (moderate emissions) and RCP 8.5 (high emissions), were used (Adefisan, 2018; Ajibola *et al.,* 2020). A quantile mapping technique was applied to correct systematic biases in the climate model outputs against the historical rainfall records from NIMET. The 95th percentile of annual maximum daily rainfall was projected to increase by 10% under RCP 4.5 and by 15% under RCP 8.5 by the 2030s. For simplicity in this initial assessment, these percentage increases were applied uniformly across the catchment, representing the median projected change. It is acknowledged that a more spatially variable rainfall projection would be desirable in future work. (3) **Population Exposure:** Future population distribution for 2034 was estimated by applying the current average annual growth rate (3.0%) to the 2023 GRID3 population data, while maintaining the existing spatial distribution pattern. This uniform growth assumption provides a conservative estimate of exposure trends in the absence of detailed migration or demographic data and is noted as a limitation of the analysis.

By running the ANN model with these future-condition inputs (2034 LULC and modified rainfall), flood hazard maps for 2034 under both RCP 4.5 and RCP 8.5 Scenarios were generated. The resulting hazard zones were then combined with the projected 2034 population grid to estimate future population exposure.

Results

Historical land use/land cover dynamics (2014-2024)

The LULC change analysis revealed profound transformations within the study period (Table 3). The most significant changes were the substantial decline in agricultural land (-337.73 km², -6.73%) and the dramatic expansion of water bodies (+229.95 km², +4.59%). A transition matrix analysis pinpointed that 217.21 km² of agricultural land was directly converted to water bodies, primarily due to the impoundment of the Zungeru Hydropower Dam reservoir. Concurrently, bare surfaces increased markedly by 243.12 km² (+4.84%), indicating extensive land clearing and degradation, while built-up areas showed a steady but modest increase of 15.49 km² (+0.31%). Landscape metrics analysis revealed an increase in patch density for bare surfaces (from 0.8 to 1.2 patches/km²) and a decrease in the largest patch index for agricultural land, indicating fragmentation. The uncertainties in change detection, derived from the classification accuracies, were propagated, resulting in an estimated error range of ±5% for the reported area changes.

Table 3: LULC change statistics for the Shiroro Dam region (2014-2024)

Class	2014 Area (km²)	2014 %	2024 Area (km²)	2024 %	Δ Area (km²)	Δ %
Agricultural Land	3463.904	69.04	3126.175	62.31	-337.729	-6.73
Bare Surface	531.147	10.59	774.269	15.43	+243.122	+4.84
Built-up Area	18.964	0.38	34.458	0.69	+15.494	+0.31
Dense Vegetation	882.234	17.58	731.405	14.58	-150.829	-3.00
Water Bodies	121.077	2.41	351.023	7.00	+229.946	+4.59
Total	**5017.33**	**100**	**5017.33**	**100**	**0.01**	**0.00**

Future land use/land cover projection for 2034

The validated CA-Markov projection for 2034 indicates a continuation of current trends, forecasting a landscape of increasing anthropogenic pressure (Table 4). The model was validated by simulating the 2024 LULC from the 2014 baseline and comparing it with the actual 2024 classification. This validation yielded a Kappa statistic of 0.78, indicating substantial agreement and supporting the reliability of the 2034 projection under a business-as-usual Scenario.

The projection results show agricultural land is projected to further reduce to 53.76% of the total area, while bare surfaces are expected to expand significantly to 25.84%, driven by ongoing land clearing for agriculture and informal settlement

development. Built-up areas are projected to increase to 0.70%, confirming the persistent, albeit slow, encroachment of settlements into vulnerable zones.

Table 4: Projected LULC for the year 2034

Class	Area (km²)	%
Agricultural Land	2,697.428	53.76
Bare Surface	1,296.713	25.84
Built-up Area	35.173	0.70
Dense Vegetation	625.961	12.48
Water Bodies	362.032	7.22
Total	**5017.307**	**100**

Flood hazard zonation and model validation

The ANN-generated flood hazard map classified the study area into distinct vulnerability zones (Table 5, Figure 3). A substantial 35.06% (1,759.19 km²) of the area was classified as 'High/Very High' vulnerability. These zones are topographically predisposed, characterized by low-lying elevations, gentle slopes, and impermeable land surfaces, predominantly coinciding with the active floodplains of the Kaduna River and its tributaries.

Table 5: Flood hazard classification for the Shiroro Dam region

Hazard Class	Area (km²)	% of Study Area
Low/Very Low	1865.534	37.18
Moderate	1356.993	27.05
High/Very High	**1759.194**	**35.06**

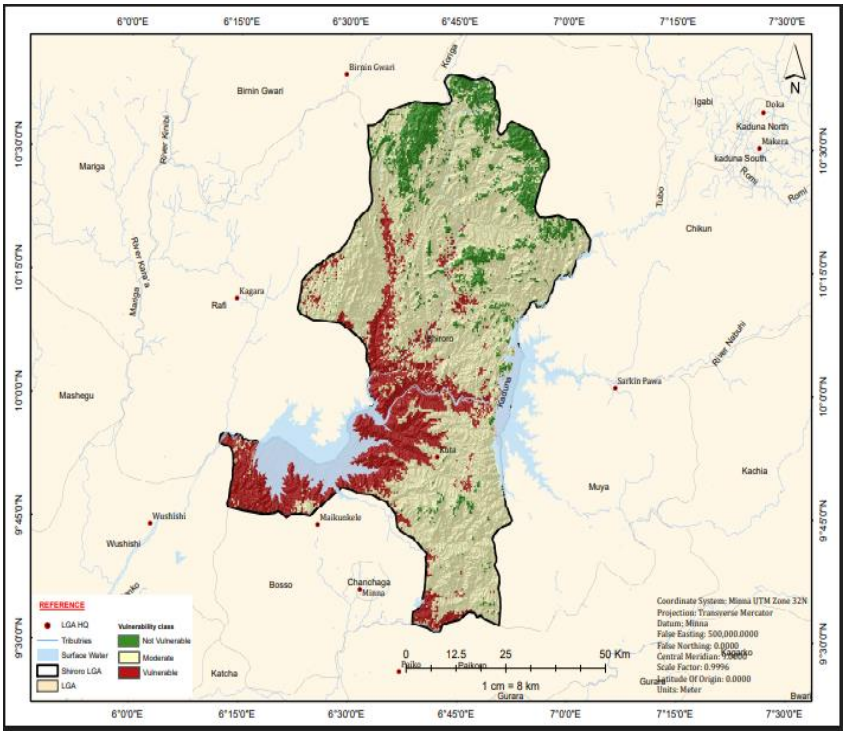

Figure 3: Spatial distribution of flood hazard zones derived from the ANN model

Validation against the 2022 observed flood event confirmed the model's high predictive capability (Table 6). The ANN significantly outperformed the baseline GIS-overlay method across all metrics with accuracy 91.6%, and Kappa Coefficient of 0.82, demonstrating its robustness. It indicates an "Almost Perfect" agreement beyond chance (Zhang *et al.*, 2016).

Table 6: Performance metrics of the ANN flood risk model

Metric	**ANN Model Performance (%)**
Accuracy	91.6
Precision	89.3
Recall	87.5
F1-Score	88.4
Kappa Coefficient	**0.82**

Projected future flood hazard and risk (2034)

The trained ANN model was applied to generate future flood hazard maps for 2034 under RCP 4.5 and RCP 8.5 Scenarios (Table 7, Figure 4). The future projections indicate a significant expansion of the 'High/Very High' flood vulnerability zone. Under RCP 4.5, the area expanded to 1,950.22 km² (38.87%), and under RCP 8.5, it expanded to 2,105.45 km² (41.97%). It is important to note that the ANN predicts susceptibility (probability of flooding) based on static conditions; it does not simulate hydrodynamic processes like inundation depth or velocity.

Table 7: Comparison of baseline and projected future (2034) flood hazard area

Hazard Class	Baseline Area (km²)	Baseline %	2034 RCP 4.5 Area (km²)	2034 RCP 4.5 %	2034 RCP 8.5 Area (km²)	2034 RCP 8.5 %
Low/Very Low	1,865.53	37.18	1,650.35	32.90	1,550.10	30.90
Moderate	1,356.99	27.05	1,416.55	28.24	1,361.78	27.14
High/Very High	1,759.19	35.06	1,950.22	38.87	2,105.45	41.97

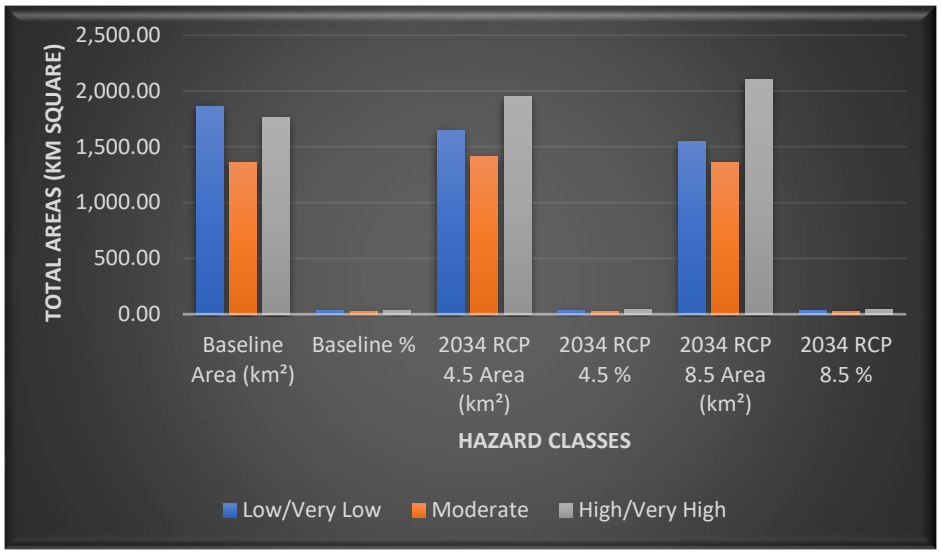

Figure 4: Projected flood hazard for 2034

Population exposure to flood risk

The spatial overlay analysis revealed a concerning convergence (Figure 5). High population density, projected to reach 7,318 persons/km² in the most vulnerable zones, is concentrated precisely within the ANN-identified 'High/Very High' flood hazard areas. This analysis pinpointed specific administrative wards, including Zungeru, Gijawa Kato, Maikunkele, and Bosso I, as high-risk hotspots where continued urban encroachment is placing a significant and growing population at direct risk. Socio-economic profiling suggests that these high-risk populations are predominantly low-income communities, smallholder farmers, and informal sector traders, who have limited capacity for adaptation and recovery.

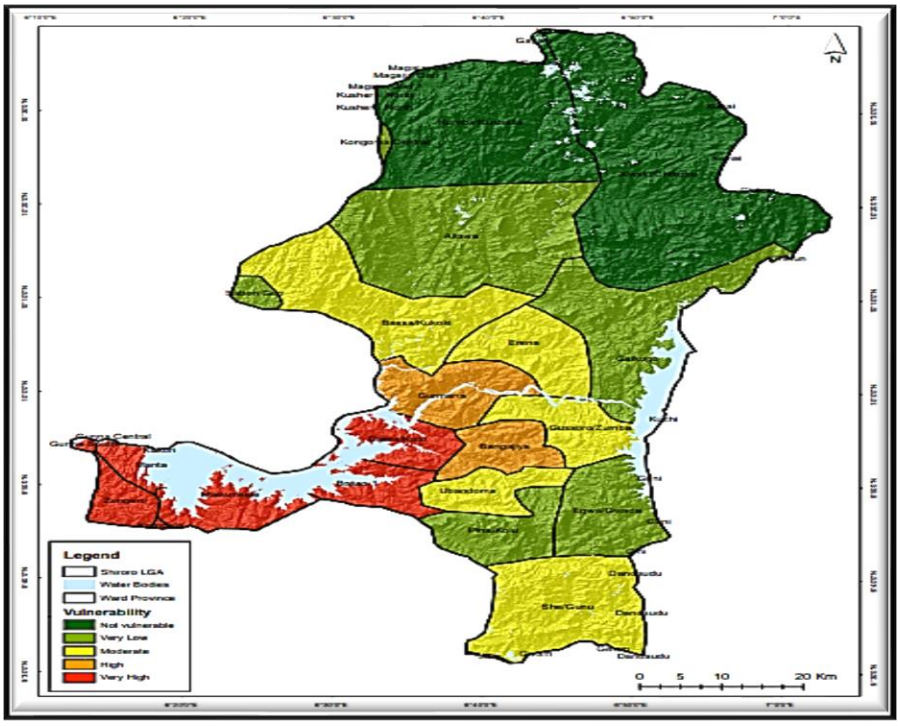

Figure 5: Map of the spatial overlay of population density and high flood hazard zones, highlighting risk hotspots

Discussion

The findings of this study, as presented in the preceding results, illustrate a complex and evolving flood risk landscape in the Shiroro Dam catchment, shaped by the interplay of land use transformation, climate change, and demographic pressures. The integrated modelling framework provides insights into both current vulnerabilities and future trajectories of risk.

The observed LULC dynamics between 2014 and 2024, detailed in Table 3, depict a landscape undergoing rapid socio-ecological transformation, primarily driven by dam infrastructure development. The most striking change is the direct inundation of 217.21 km² of agricultural land, contributing to a net loss of 6.73% of this land cover class. This conversion, visually evident in the expansion of water bodies by 4.59%, represents a severe livelihood crisis and a tangible threat to regional food security, a finding consistent with the trade-offs associated with large dams where local populations often bear disproportionate costs (Adepoju *et al.,* 2020; UNEP, 2021). Concurrently, the marked increase in bare surfaces (+4.84%) signals widespread land degradation, which diminishes infiltration capacity and exacerbates surface runoff, thereby amplifying the physical flood hazard (McGrane, 2016). The steady increase in built-up area (+0.31%), while modest in total area, confirms the persistent encroachment of settlements into the catchment.

The application and validation of the Artificial Neural Network model mark a significant methodological advancement. As shown in Table 6 and spatially represented in Figure 3, the ANN model demonstrated exceptional performance (Accuracy: 91.6%, Kappa: 0.82), significantly outperforming the traditional GIS-overlay baseline method. This superiority stems from the ANN's inherent capacity to model the non-linear and complex interactions between the five geo-environmental causative factors, effectively delineating flood-prone zones that align with the topographically predisposed active floodplains of the Kaduna River. This result corroborates the growing advocacy for machine learning in geohazard assessment (Mosavi *et al.,* 2018; Shahabi *et al.,* 2021) and provides a robust, data-driven foundation for the subsequent forecasting steps.

The integration of future Scenarios reveals a concerning trajectory for flood risk. The CA-Markov projection for 2034 (Table 4) forecasts a continuation of current land-use trends, with further reduction of agricultural land and expansion of bare surfaces. When these future LULC conditions and modified climate inputs were fed into the trained ANN, the resulting hazard maps (Figure 4 and Table 7) project a significant expansion of the 'High/Very High' flood vulnerability zone. Under the RCP 4.5 scenario, this zone expands to 38.87% of the study area, and under the high-emission RCP 8.5 scenario, it expands to 41.97%. This expansion demonstrates that the ongoing anthropogenic land-use change is actively amplifying the physical flood hazard, an effect that may equal or exceed the influence of changing climate patterns in the short term. This finding highlights the specific amplifying role of dam-

induced landscape transformation on flood susceptibility.

The most critical finding emerges from the spatial integration of hazard and exposure. The overlay analysis presented in Figure 5 reveals a dangerous convergence: high population density, projected to reach 7,318 persons/km², is concentrated precisely within the ANN-identified 'High/Very High' flood hazard zones. This compound risk scenario effectively identifies specific administrative wards as high-risk hotspots. The identification of 35.06% of the study area as highly vulnerable in the baseline (Table 5), coupled with this dense human settlement, presents a clear and present danger that necessitates an urgent paradigm shift from reactive disaster response to proactive risk governance.

Several limitations must be acknowledged when interpreting these results. The future climate integration used a uniform percentage increase for rainfall, a simplification that future work should refine with spatially variable projections. Population growth was projected uniformly, which may not capture internal migratory patterns. Furthermore, while the ANN excelled at susceptibility mapping, it does not simulate hydrodynamic processes like inundation depth or velocity, which are crucial for detailed impact assessment. Finally, the CA-Markov model, despite good validation, operates under a business-as-usual assumption and may not capture sudden policy or economic shifts.

Despite these limitations, the integrated framework provides a powerful and transferable tool. The results offer a strong evidenced base for targeted interventions. They highlight that effective flood risk management in dam-regulated catchments like Shiroro requires an integrated policy response focused on stringent land-use governance in high-hazard zones, improved early warning systems informed by such susceptibility maps, and climate-resilient urban planning to avert the forecasted increase in risk.

Conclusion

This study successfully developed and validated a dynamic, integrative ANN-based framework for forecasting urban flood risk in the dam-regulated Shiroro catchment. The research demonstrates that the synergy of remote sensing, urban growth modelling, and machine learning provides a far more accurate and proactive tool for flood risk assessment than conventional methods. The key conclusions are: (i) Dam infrastructure has been a primary driver of significant landscape change, resulting in the direct loss of farmland and alteration of local hydrology (ii) The ANN model proved highly robust and accurate in delineating flood-prone areas, effectively capturing the complex, non-linear relationships between causative factors (iii) The application of the framework to 2034 projects a significant expansion of the high-hazard zone under both climate Scenarios, indicating that both the physical hazard and population exposure will intensify.

The study has limitations, including assumptions in climate and population projections and the static nature of the susceptibility model. Nevertheless, the methodology is transferable to other dam-affected catchments. We strongly recommend operational adoption by agencies such as the Niger State Emergency Management Agency (NSEMA) and the Nigerian Hydrological Services Agency (NIHSA) for integrating the ANN model into their decision-support systems for regular flood forecasting, early warning, and land-use planning. This approach can significantly contribute to achieving Sustainable Development Goals 11 (Sustainable Cities) and 13 (Climate Action) in vulnerable regions.

Acknowledgements

The authors acknowledge the Department of Surveying and Geoinformatics at the Federal University of Technology, Minna, for providing academic support for this research. We also extend our gratitude to the USGS, DLR, GRID3, NASRDA, NIMET, and NEMA for providing the foundational data used in this study.

References

Abubakar, I. R., Dano, U. L., & Bala, H. (2018). Unregulated urban expansion and flooding in Minna, Nigeria. *Environmental Hazards, 17*(2), 145-163.

Adefisan, E. A. (2018). Climate change projections over West Africa using RCA4. WASCAL Technical Report, 1-45.

Ajibola, F. O., Taiwo, O. J., & Aguda, A. S. (2020). Effects of climate change on extreme rainfall events over Niger River Basin, Nigeria. *Journal of Water and Climate Change*, 11(4), 1456-1474. https://doi.org/10.2166/wcc.2019.295

Adepoju, K. A., Lawal, M., & Oladejo, S. (2020). Land use/land cover dynamics around Shiroro Dam, Nigeria: Implications for sustainable management. *Remote Sensing Applications: Society and Environment, 18*, 100308.

Adesina, E. A., Musa, A., Ajayi, O. G., Odumosu, J. O., Opaluwa, Y. D., & Onuigbo, I. C. (2021). Comparative assessment of SRTM and UAV-derived DEM in flood modelling. *Environmental Technology and Science Journal, 12*(2), 58-70. https://doi.org/10.4314/etsj.v12i2.6

Adesina, E. A., Odumosu, J. O., Ajayi, O. G., Musa, A., Onuigbo, I. C., & Adesiji, A. R. (2025). Evaluating the impact of the Spatial resolution of digital elevation models on flood modelling. *Water Resource Management*, 39, 5359–5390 (2025). https://doi.org/10.1007/s11269-025-04206-6

Berhane, G., Tehrany, M. S., & Pham, B. T. (2024). Advances in machine learning for flood hazard mapping. *Science of The Total Environment, 896*, 165223.

Dottori, F., Szewczyk, W., Ciscar, J.C., Zhao, F., Alfieri, L., Hirabayashi, Y., Bianchi, A., Mongelli, I., Frieler, K., Betts, R. A., & Feyen, L. (2018). Increased human and economic losses from river flooding with anthropogenic warming. *Nature Climate Change, 8*(9), 781-786.

EM-DAT. (2023). *The international disaster database*. Centre for Research on the Epidemiology of Disasters (CRED), Universite Catholique de Louvain. Retrieved from https://www.emdat.be

Gupta, H., Anderson, M., & Kumar, R. (2020). Urbanization impacts on flood risk in sub-Saharan Africa. *Water, 12*(2), 325.

Intergovernmental Panel on Climate Change (IPCC). (2022). *Climate change 2022: Impacts, adaptation and vulnerability*. Cambridge University Press.

Jongman, B., Ward, P. J., & Aerts, J. C. J. H. (2012). Global exposure to river and coastal flooding: Long term trends and changes. *Global Environmental Change*, 22(4), 823-835.
https://doi.org/10.1016/j.gloenvcha.2012.07.004

McGrane, S. J. (2016). Impacts of urbanization on hydrological and water quality dynamics, and urban water management: A review. *Hydrological Sciences Journal, 61*(13), 2295-2311.

Mosavi, A., Ozturk, P., & Chau, K. (2018). Flood prediction using machine learning models: Literature review. *Water, 10*(11), 1536.

Nkwunonwo, U. C., Whitworth, M., & Baily, B. (2020). A review of the current status of flood risk modelling in Nigeria. *Natural Hazards, 104*, 123-146.

Lu, D., & Weng, Q. (2007). A survey of image classification methods and techniques for improving classification performance. *International Journal of Remote Sensing*, 28(5), 823-870.
https://doi.org/10.1080/01431160600746456

Olanrewaju, O. A., Abubakar, I. R., & Adebayo, O. S. (2019). Urbanization and flood risk in the Niger Basin. *Environmental Monitoring and Assessment*, 191(4), 242.

Shahabi, H., Shirzadi, A., Ronoud, S., Asadi, S., Pham, B. T., Mansouri, S., Clague, J. J., Geiss, C., Ghorbanzadeh, O., & Bahrami, S. (2021). Flash flood susceptibility mapping using a novel deep learning model based on deep belief network, back propagation and genetic algorithm. *Geoscience Frontiers, 12*(3), 101100.

United Nations Environment Programme (UNEP). (2021). *Dams and development: Relevant practices for improved decision-making*.

United Nations Office for Disaster Risk Reduction (UNDRR). (2017). *Global assessment report on disaster risk reduction*. United Nations.

Vanbelle, S., Engelhart, C. H., & Blix, E. (2024). A comprehensive guide to study the agreement and reliability of multi-observer ordinal data. *BMC medical research methodology*, 24(1), 310.

Zhang, J., Wang, Z., & Xu, Y. (2016). Accuracy assessment in remote sensing: Kappa statistics explained. *Remote Sensing Letters, 7*(9), 882-891.